

Effects of a slowdown warning system in mixed communication environments : A macroscopic study

Animesh Chakravarthy, Jaime Peraire, Eric Feron

Abstract—Current ACC vehicles do not provide the driver with advance information of events occurring far ahead of him/her. In this paper, we discuss the concept of a slowdown warning system in automobiles, and analyze the same using PDE models. If a driver on a highway progresses abnormally slowly and/or generates large negative velocity gradients on the highway (thereby posing a hazard to the vehicles behind him/her), then, with such a system, the cars behind him/her are provided advance information of this. This advance information gives the drivers additional time to react, in anticipation of an impending slow-down, and this helps to smoothen the velocity gradients. Furthermore, and more importantly, it is seen that even if only a fraction of the cars in a platoon are equipped with such an advance warning system, this can still be sufficient to weaken the velocity gradients even in the unequipped cars. In this paper, we demonstrate this through simulations on PDE models assuming finite communication wave propagation speeds through the equipped cars.

I. INTRODUCTION

Rear end collisions are a major cause of multiple car crashes, especially during bad weather conditions [1], [2], [3], [4]. The cause for such crashes is that each driver gets warned of an impending slowdown ahead, only when the brake-lights of a car/group of cars immediately in front of him/her, turn on. This is particularly true during poor visibility conditions, and/or while driving behind a large vehicle, when a driver is unable to look too far ahead, as he/she otherwise normally would have. So, if we consider a situation when there is a large negative velocity gradient occurring at some point on the highway, then information of the existence of such a gradient is propagated from car to car in a staggered fashion (Figure 1(a)), as the brake-lights of each car come on, one after the other. This mode of information propagation is often too slow, and as a consequence, these large velocity gradients travel along the highway, mostly unattenuated. The stronger this velocity gradient, the higher the discomfort experienced by a driver, as this gradient passes through him/her - and the higher the possibility of occurrence of a pileup crash.

There exists an important analogy between the occurrence of car pile-up crashes and the shock waves occurring in compressible flow dynamics. The earliest such discussion of shock waves in traffic flow dynamics appeared in [5].

In this paper, we discuss a means to alleviate the possibility of car pile-up crashes. For this, we discuss a slowdown warning concept, whereby cars are equipped with a slowdown warning system. A car equipped with such a system has

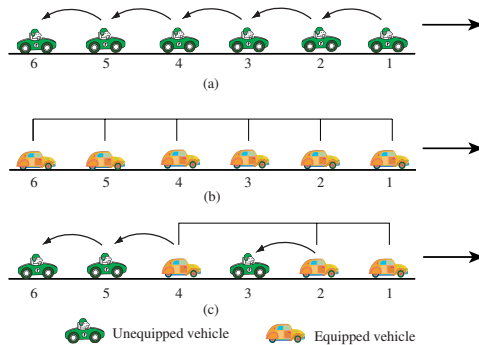


Fig. 1. Propagation of slowdown information in cases (a), (b) and (c).

the ability to (i) Automatically transmit a slowdown warning signal whenever it anticipates the existence of a region of large negative velocity gradient ahead, or its velocity becomes dangerously low for highway driving conditions, and (ii) Receive a slowdown warning signal, and alert the driver accordingly, if it deems the signal to be relevant. With such a system, one can achieve faster information propagation speeds; so that cars further behind are warned of the existence of a hazard ahead, earlier than they otherwise would have. This advance information enables the drivers to react appropriately and slow down in order to avoid the crash. Figure 1(b) shows a schematic representation of the existence of a network of equipped vehicles, that enable faster information propagation amongst themselves.

In a real-life scenario, however, it would be unrealistic to assume that all the cars in a platoon will indeed be equipped with a slow-down warning system. It is pertinent therefore, to examine the influence of such a system, when only a (randomly selected) fraction of the total number of cars in the platoon are equipped with the system. In this case, information is propagated as in Figure 1(c). The figure shows a schematic representation of networks of equipped vehicles, scattered amongst the unequipped vehicles.

The use of inter-vehicle communication for enhancement of vehicle safety has been discussed, *e.g.*, in [9], [13], [10], [11], [12] though not in the context of alleviating car pile-up crashes with partial inter-vehicle communication. While there has been recent research activity on mixed systems (comprising of semi-automated and manual vehicles), [21], [22], these systems do not assume inter-vehicle communication. We therefore believe that there is value in the analysis of mixed systems with partial inter-vehicle communication, involving information propagation as in Fig. 1(c). This paper

is a step in that direction, and addresses the specific issues of car pile-up crashes, shock waves and their alleviation. In [23], [24], [25], we discussed results of some simulation studies using microscopic and cellular automaton models incorporating the slowdown warning system and details of road test results that were performed after equipping cars with the slowdown warning system.

The use of macroscopic models for studying traffic flows has a fairly long history. The Lighthill-Whitham-Richards (LWR) model [6], [5] represents the earliest use of macroscopic models to represent traffic flow. The LWR model is basically a first order model that is based on a gas dynamic-like continuity equation (representing the conservation of cars). Subsequently, second order models have been developed, for example, the Payne-Whitham model [7]. Prigogine and Herman [18] developed traffic flow equations based on the Boltzmann equation, which have been further refined by Paveri-Fontana [19]. Based on Paveri Fontana's equations, Helbing then derived a (gas dynamic based) third order macroscopic traffic model [15] (this model included an equation for the velocity variance), and also a second order traffic model [16], that is anisotropic in nature. Helbing also derived a gas dynamic based two species traffic model where the two species were cars and trucks [16], as also did Hoogendoorn and Bovy [17]. There have also been papers on analysis of stability in traffic flows[20]. In this paper, we adapt the Helbing model [16] to a situation wherein the two species comprise vehicles equipped with the ability to receive advance far-ahead information, interspersed with unequipped vehicles that are capable of sensing only local information. We also adapt the Helbing model appropriately in order to account for a finite speed of information propagation among the equipped vehicles.

The goal of this paper is to examine how the slowdown warning system can weaken a shock, even in a mixed sensing environment wherein there is only a partial equipage of the slowdown warning system. The presence of some equipped vehicles (who, in some sense, receive advance information of the possibility of a shock ahead before it actually reaches them) can help in diminishing the strength of the shock (even among the unequipped vehicles), thereby smoothing the traffic flow. This paper is organized as follows. Section II discusses the macroscopic model used and demonstrates simulation results showing initial conditions under which a shock propagates through the traffic. Section III then discusses the macroscopic model used in a situation of partial equipage, and with a finite speed of information propagation among the equipped vehicles; and demonstrates simulation results showing the strength of the shock wave in both - the equipped and unequipped vehicles under the same initial conditions, and for varying equipages. Section IV presents the conclusions.

II. ALL VEHICLES UNEQUIPPED : MODEL AND SIMULATIONS

We use the model derived by Helbing [16], which in turn, has been inspired by the gas kinetic based models derived

by Prigogine and Herman [18], and Paveri Fontana [19]. Defining $\rho(x, t)$ as the average density, $V(x, t)$ as the average velocity and $\theta(x, t)$ as the velocity variance in the region $[x - dx/2, x + dx/2]$, the following macroscopic equations are obtained :

$$\frac{\partial \rho}{\partial t} + \frac{\partial(\rho V)}{\partial x} = 0 \quad (1)$$

$$\frac{\partial(\rho V)}{\partial t} + \frac{\partial(\rho V^2 + \rho \theta)}{\partial x} = \rho \frac{V^{eq} - V}{\tau} \quad (2)$$

The above hierarchy of equations is closed by assuming that $\theta = A(\rho)V^2$. Furthermore, $V_e(x, t)$ represents the average equilibrium velocity and is given by :

$$V^{eq}(x, t) = V^o - P(\rho_a)B\rho\tau\theta \quad (3)$$

where V^o represents the average desired velocity, τ represents the average relaxation time, ρ_a represents the average density computed at the interaction point $x_a = x + \gamma(l + VT)$, with $l = 1/\rho_{max}$ representing the average vehicle length (ρ_{max} represents the maximum vehicle density), T denotes the average time headway that vehicles try to maintain in the limit of maximum density, and $\gamma \in [1, 3]$ represents an anticipation factor. The factor $P(\rho)$ that takes into effect both the probability of overtaking, as well as the existence of a finite interaction-free space, is defined as $P(\rho) = \frac{V^o \rho T^2}{\tau A(\rho_{max})(1 - (\rho/\rho_{max})^2)}$. The factor B that takes into account the anisotropic interaction effects, is given as

$$B(\delta_v) = \delta_v \frac{e^{-\delta_v^2/2}}{\sqrt{2\pi}} + (1 + \delta_v^2) \int_{-\infty}^{\delta_v} \frac{e^{-y^2/2}}{\sqrt{2\pi}} dy \quad (4)$$

where $\delta_v = (V - V_a)/\sqrt{\theta + \theta_a}$ with V_a and θ_a representing the average velocity and velocity variance computed at the interaction point x_a . The following values have been assumed for the numerical data (when all vehicles are unequipped) :

Average desired velocity $V^o = 110 \text{ km/hour}$ (This corresponds to a highway speed limit that a driver would like to maintain, if the road was empty)

Average relaxation time $\tau = 15 \text{ sec}$

Maximum vehicle density $\rho_{max} = 160 \text{ vehicles/km/lane}$

Average time headway $T = 1 \text{ sec}$

$A(\rho)$ which is the density dependent pre-factor has the profile given in Figure 2 [16]. Using these values, the following curve representing the variation of average equilibrium velocity with density, is obtained (Figure 3) [16].

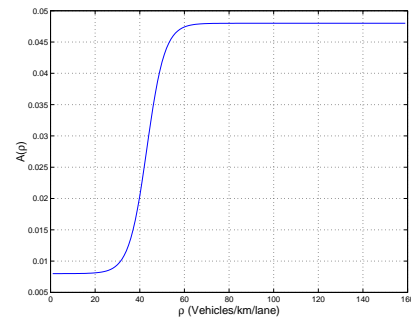


Fig. 2. Variance Pre-factor Profile

A good prototype of an initial condition used to test the influence of the slowdown warning system in a mixed equipage scenario, is the Riemann Problem. The Riemann

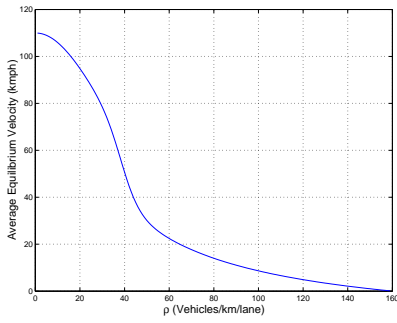


Fig. 3. Equilibrium Average Velocity Profile

Problem represents an initial condition comprising of a left state and a right state joined by a discontinuity, in each of the dependent variables, with the discontinuity occurring at the same spatial location for both variables. The left states are denoted by ρ_L and V_L , while the right states are denoted by ρ_R and V_R respectively.

In the Riemann Problems that we will consider, we will assume that $\rho_L < \rho_R$ and $V_L > V_R$. It can be seen that a large drop in average velocity, occurring over a short distance (in other words, a large negative spatial velocity gradient) is indicative of a potentially unsafe driving situation. We choose $\rho_L = 15$ vehicles/km/lane and $\rho_R = 140$ vehicles/km/lane. We assume that ρ changes from ρ_L to ρ_R over a length of 200 meters, which appears as a shock over a length scale of 10 km. Additionally, we will assume that the left and right states are both in their respective equilibrium (when all vehicles are unequipped). From Figure 3, it can be seen that this implies that $V_L = 105.67$ kmph and $V_R = 3.17$ kmph. We use boundary conditions as follows : $\rho(0, t) = \rho(0, 0)$; $V(0, t) = V(0, 0)$.

Figure 4 then shows the average density and average velocity profiles as a function of space and time, when all the vehicles are unequipped. It can be seen that the initial large negative velocity gradient propagates, almost unattenuated, backwards along the highway. The wave speed at which it propagates is found as $\frac{\rho_L V_L - \rho_R V_R}{\rho_L - \rho_R} = -9.1 \text{ kmph}$. Figure 5 shows the average driver trajectories on a space-time plane. On this figure too, the shock-like behavior is clearly seen.

The presence of a large negative gradient on an initial velocity condition can also be seen as a large negative perturbation on $\frac{\partial V}{\partial x}$. As can be seen from Figure 14, with all vehicles unequipped, $\frac{\partial V}{\partial x}$ attenuates in magnitude initially for a short while, only very slightly, and then propagates along unattenuated. If we define $\|\frac{\partial V}{\partial x}\|_\infty = \max_x \frac{\partial V}{\partial x}$ at a given time t , then the time history of $\|\frac{\partial V}{\partial x}\|_\infty$ is shown in Figure 15. In the next section, we will analyze how the same initial condition evolves in a situation of partial equipage with the slowdown warning system.

A second initial condition of interest is one that is initially continuous, but then propagates with time, in a manner such as to eventually form a shock. In other words, the initial (decreasing) average velocity profile steepens with time. It is of interest to see how a partial equipage of the slowdown

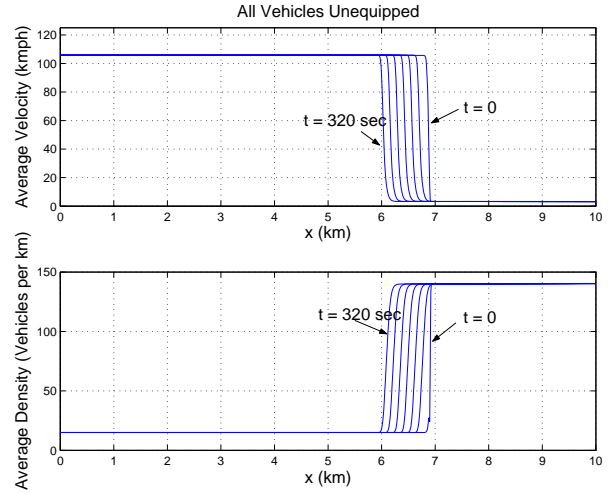


Fig. 4. Average Velocity and Density profiles (All vehicles unequipped) for the Riemann Problem

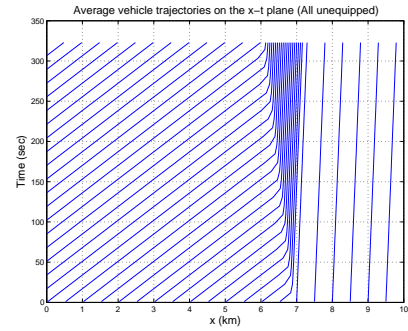


Fig. 5. Average Vehicle trajectories on the x-t plane (All vehicles unequipped) for the Riemann Problem

warning system can help arrest the wave steepening scenario that can exist (when all vehicles are unequipped), and to then parametrize this effect as a function of varying equipage.

For this purpose, we invoke an initial condition with identical left and right states as before, i.e. $\rho_L = 15$ vehicles/km/lane, $\rho_R = 140$ vehicles/km/lane and $V_L = 105.67$ kmph, $V_R = 3.17$ kmph; but instead of joining them by a discontinuity, we now join ρ_L to ρ_R by a gradual transition, so that the average density increases from ρ_L to ρ_R over a span of 2 km. The average velocity varies from V_L to V_R in a manner so that the average velocity is in equilibrium with the average density at each x .

Figure 6 then shows the average density and average velocity profiles as they evolve with time, from the above initial condition. It is seen that the top portion of the velocity wave (and the bottom portion of the density wave) move forward relative to the highway, i.e. they have positive wave velocity; while the bottom portion of the velocity wave (as also the high density part of the density wave) move backwards, with a negative wave velocity. This kind of wave motion (wherein different parts of the wave have wave velocities of opposite signs), leads to further and further steepening of the wave, until eventually a shock is formed,

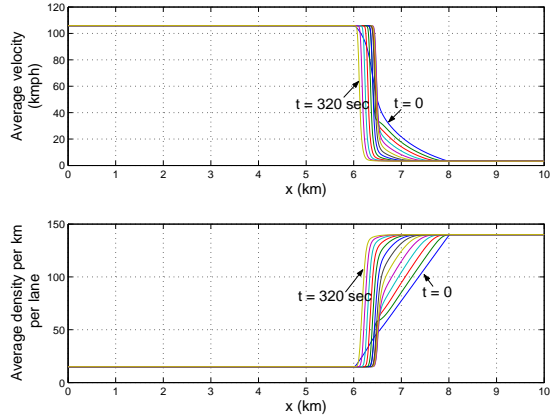


Fig. 6. Average velocity and density profiles (all vehicles unequipped) for a continuous initial condition

that then moves backwards as a whole. The evolution of $\|\frac{\partial V}{\partial x}\|_{\infty}$ showing the gradual steepening of the wave is given in Figure 19, while Figure 18 gives the magnitude of ΔV , which represents the velocity change that occurs over the region where the value of $\frac{\partial V}{\partial x}$ is less than -100 kmph/km. It is seen that over a span of approximately 5 minutes, ΔV increases to almost 100 kmph, which makes it almost identical to the initial condition of the first case we explored.

III. PARTIAL EQUIPAGE OF THE SLOWDOWN WARNING SYSTEM : MODEL AND SIMULATIONS

We now intend to test the above two initial conditions in a scenario of mixed equipage, schematically depicted in Figure 7. To this end, we assume that at $t = 0$, the average velocity of the equipped vehicles is identical to that of the unequipped vehicles. $\rho_U(x, t)$, $V_U(x, t)$ are used to represent the average density and average velocity of the unequipped vehicles, while $\rho_E(x, t)$ and $V_E(x, t)$ represent the average density and average velocity of the equipped vehicles. To test the effect of varying equipage, we vary ρ_U and ρ_E , so that $\frac{\rho_E(x)}{\rho_U(x) + \rho_E(x)}$ represents the percentage of equipage at each x , and we keep $\rho_U(x, 0) + \rho_E(x, 0) =$ a constant which is equal to the density of vehicles when they were all unequipped. In other words, $\rho_{UL}(x, 0) + \rho_{EL}(x, 0) = \rho_L(x, 0)$; $\rho_{UR}(x, 0) + \rho_{ER}(x, 0) = \rho_R(x, 0)$; $V_{UL}(x, 0) = V_{EL}(x, 0)$; $V_{UR}(x, 0) = V_{ER}(x, 0)$, where the values for ρ_L , ρ_R , V_L and V_R correspond to the values when all vehicles were unequipped (as discussed in the previous section).

The following macroscopic equations for the mixed equipage scenario are used :

$$\frac{\partial \rho_U}{\partial t} + \frac{\partial(\rho_U V_U)}{\partial x} = 0 \quad (5)$$

$$\frac{\partial \rho_E}{\partial t} + \frac{\partial(\rho_E V_E)}{\partial x} = 0 \quad (6)$$

$$\frac{\partial(\rho_U V_U)}{\partial t} + \frac{\partial(\rho_U V_U^2 + \rho_U \theta_U^2)}{\partial x} = \frac{V_U^{eq} - V_U}{\tau} \quad (7)$$

$$\frac{\partial(\rho_E V_E)}{\partial t} + \frac{\partial(\rho_E V_E^2 + \rho_E \theta_E)}{\partial x} = \frac{V_E^{eq} - V_E}{\tau} \quad (8)$$

where $V_E^{eq}(x, t)$ represents the average equilibrium velocity of the equipped vehicles and is given by :

$$V_E^{eq}(x, t) = V_E^o - PB_{EU}\rho_U\tau\theta_U - PB_{EE}\rho_E\tau\theta_E \quad (9)$$

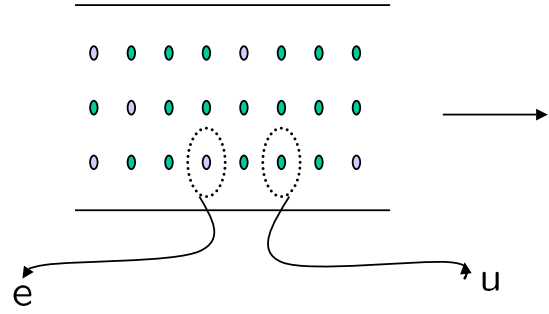


Fig. 7. Schematic multi-vehicle scenario comprising of unequipped and equipped vehicles

and where $V_U^{eq}(x, t)$ represents the average equilibrium velocity of the unequipped vehicles and is given by :

$$V_U^{eq}(x, t) = V_U^o - PB_{UE}\rho_E\tau\theta_E - PB_{UU}\rho_U\tau\theta_U \quad (10)$$

V_U^o and V_E^o denote the average desired velocities of the unequipped and equipped vehicles respectively.

$P = \frac{(\rho_U + \rho_E)T^2 V_{avg}^o}{\tau A \rho_{max} (1 - ((\rho_U + \rho_E) / \rho_{max})^2)}$ and $V_{avg}^o = (\rho_U V_U + \rho_E V_E) / (\rho_U + \rho_E)$. θ_U and θ_E represent the velocity variances of the unequipped and equipped vehicles respectively, and it is assumed that $\theta_U = A(\rho_U + \rho_E)V_U^2$ and $\theta_E = A(\rho_U + \rho_E)V_E^2$. Also, $B_{ue}, B_{ee}, B_{eu}, B_{uu}$ have the same form as B_{in} Equation (4) except for the fact that we now have $B_{ue} = B(\delta v_{ue})$; $B_{uu} = B(\delta v_{uu})$; $B_{eu} = B(\delta v_{eu})$; $B_{ee} = B(\delta v_{ee})$; where $\delta v_{ue} = (V_u - V_{ea}) / \sqrt{(\theta_u + \theta_{ea})}$; $\delta v_{eu} = (V_e - V_{ua}) / \sqrt{(\theta_e + \theta_{ua})}$; $\delta v_{uu} = (V_u - V_{ua}) / \sqrt{(\theta_u + \theta_{ua})}$; $\delta v_{ee} = (V_e - V_{ea}) / \sqrt{(\theta_e + \theta_{ea})}$.

The above equations are similar to the equations used in [16] when the two species of vehicles assumed were cars and trucks, and in that context, it was assumed that the desired velocities of the cars and trucks remained constant for all time. In our context however, we assume that the equipped vehicles change their desired velocities instantaneously on receipt of the communication wave - we therefore define an additional variable $\gamma(x, t)$ and add in the following additional equations:

$$V_E^o = \gamma(x, t)V_{Efinal}^o + (1 - \gamma(x, t))V_{Einitial}^o \quad (11)$$

$$\frac{\partial \gamma}{\partial t} + a \frac{\partial \gamma}{\partial x} = 0, \quad (12)$$

where $\gamma(x, t)$ is a Heaviside step function defined such that $\gamma(x, t) = 0$ for that x (part of the highway that has not received the communication wave by time t), and $\gamma(x, t) = 1$ for all other x . Equation (11) thus implies that the moment an equipped vehicle at x receives the slowdown warning signal at a time t , its desired velocity changes instantaneously from its initial value $V_{Einitial}^o$ (which is assumed to be the same as V_U^o - the desired velocity of the unequipped vehicles) to a final value of V_{Efinal}^o (which is assumed to be approximately equal to the average velocity occurring at the degraded point far ahead, where a hazard has occurred). Equation (12) is a PDE that postulates the evolution of $\gamma(x, t)$ and in which $a < 0$ represents the communication speed. The boundary condition $\gamma(10, t) = 1$ is imposed.

We note that alternative formulations are also possible. For instance, if we assume that information of the location of the hazard is also broadcast to the equipped vehicles (along with the warning signal), then it is reasonable to assume that the driver of the equipped vehicle will adapt his desired velocity (as a function of distance to the hazard) so that he attains his final desired velocity by the time he reaches the location of the hazard. In this case, we could rewrite Equation (11) as

$$V_E^o = \gamma(x, t) \left[(1 - \alpha(x, t)) V_{E\text{final}}^o + \alpha(x, t) V_{E\text{initial}}^o \right] + (1 - \gamma(x, t)) V_{E\text{initial}}^o \quad (13)$$

where $\alpha(x, t)$ is a function that evolves according to the PDE

$$\frac{\partial \alpha}{\partial t} + V_E \frac{\partial \alpha}{\partial x} = -\frac{V_E}{d_0}, \quad (14)$$

with d_0 representing the average distance of an equipped car to the location of the hazard, when it first received the warning signal, and the initial condition on α is specified such that $\alpha(x, 0) = 1$ for all x to the left of the hazard, and $\alpha(x, 0) = 0$ for all x to the right of the hazard. The boundary condition on α would be $\alpha(0, t) = 1$. For the purposes of this paper, we assume that the change in the desired velocity of the equipped vehicle occurs instantaneously, i.e. Equations (11) and (12) are employed.

For the first initial condition, we assume an average communication speed of 25 kmph, relative to the highway, and moving backwards. Such a communication speed can be achieved from an initial velocity of about 100 kmph, if the velocity threshold is approximately 25 kmph, coupled with a transmission range of about 500 meters. In other words, everytime an equipped vehicle (that is travelling at an initial velocity of around 100 kmph) receives the warning signal and begins to slow down (in anticipation of the hazard ahead); and then throws the signal back by 500 meters once its velocity falls below a threshold of 25 kmph; then this will result in a communication wave travelling backwards at around 25 kmph (on an average), relative to the highway.

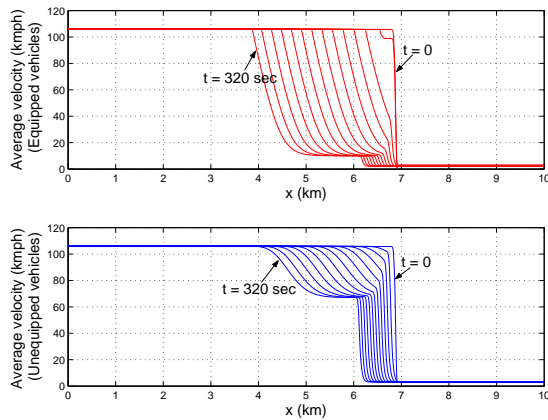


Fig. 8. Average Velocity profiles of Equipped and Unequipped Vehicles (5% equipage) for the Reimann Problem

Figure 8 shows the average velocity profiles of the equipped and unequipped vehicles respectively (for a 5% equipage scenario), while Figure 9 shows the average density

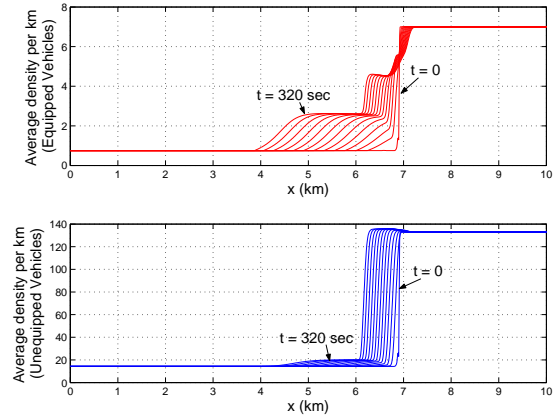


Fig. 9. Average Density profiles of Equipped and Unequipped Vehicles (5% equipage) for the Reimann Problem

profiles of the same. It can be seen that as the communication wave propagates through the equipped vehicles, causing them to slow down, the unequipped vehicles are also forced to slow down earlier than they otherwise would have (they thus receive indirect information of the hazard ahead). The wave velocity of the top portion of the average velocity of the unequipped vehicles has now become negative (it was formerly positive when they had no equipped vehicles among their midst); and this in turn has led to a lower magnitude of the average velocity shock experienced by the unequipped vehicles. Figure 10 shows the average vehicle trajectories of the equipped and unequipped vehicles, on a $x-t$ plane. The propagation of the communication wave is also seen.

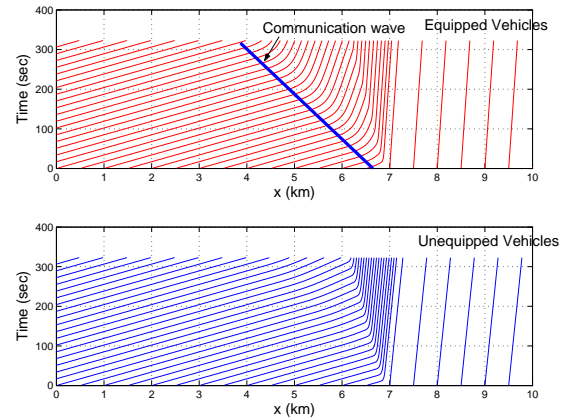


Fig. 10. Average Vehicle trajectories of Equipped and Unequipped Vehicles on the $x-t$ plane (5% equipage) for the Reimann Problem

Figure 11 then demonstrates the average velocity profiles of the unequipped vehicles, for varying degrees of equipage, while Figure 12 demonstrates the magnitude of the velocity shock as a function of time, for the different equipages. It is seen from Figure 12 that the largest reduction in ΔV that can occur with a 5% increase in equipage, occurs in the 0 – 5% range. With 10% equipage, the velocity shock magnitude in the unequipped vehicles is reduced almost by a factor of one-half, for equipages above 15%, the magnitude of benefit

obtained (as measured from the reduction in shock strength of the unequipped vehicles per unit increase in the density of the equipped vehicles), is not significantly increased. This behavior is also manifested in Figure 13 as also Figure 15, which demonstrates $\|\frac{\partial V_u}{\partial x}\|_{\infty}$, as a function of time.

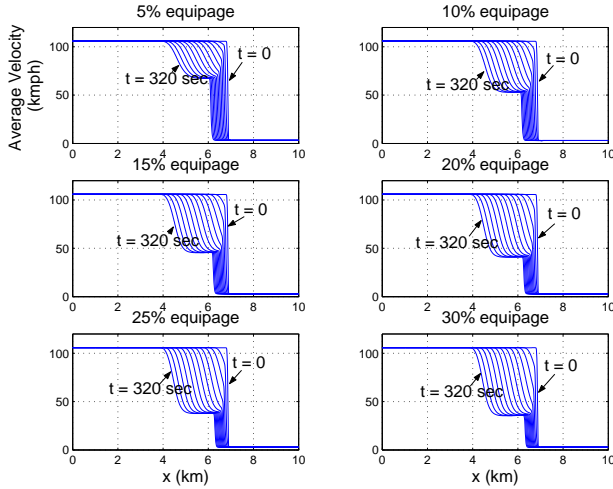


Fig. 11. Average Velocity profiles of unequipped vehicles with varying equipages for the Riemann Problem

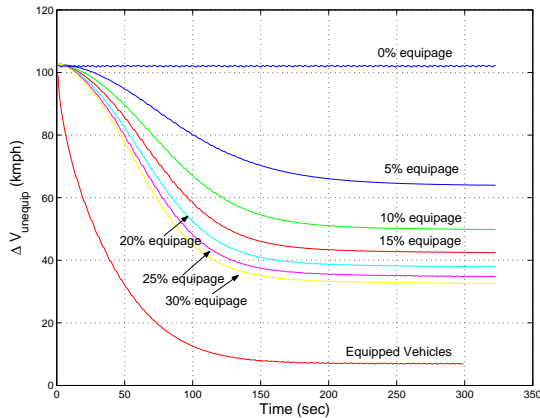


Fig. 12. Magnitude of Δv for different percentages of equipage for the Riemann Problem

After our discussion on the Riemann Problem, we now direct our attention towards the second initial condition studied earlier, i.e. a situation wherein an initially continuous gradient, evolved with time, to get progressively steeper and eventually appear like a discontinuity. In this case, we test two different scenarios : in the first, we assume that information of the existence of a velocity gradient is made available to the equipped vehicles residing to the left of the point $x = 6km$, at $t = 0$; while in the second, we assume that information of low velocity conditions ahead is made available to the equipped vehicles residing to the left of the point $x = 8km$. Again, in either case, the communication wave is assumed to travel at a constant speed of 25 kmph, in the backward direction; this time originating from $x = 6km$, at $t = 0$ (in the first case) and originating from $x = 8km$, at

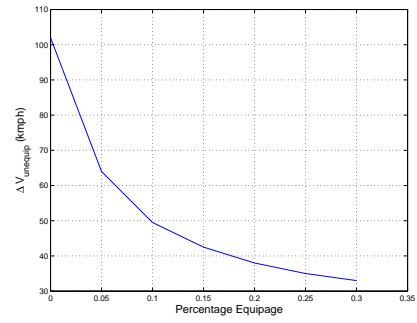


Fig. 13. Magnitude of ΔV_u at steady state for different percentages of equipage for the Riemann Problem

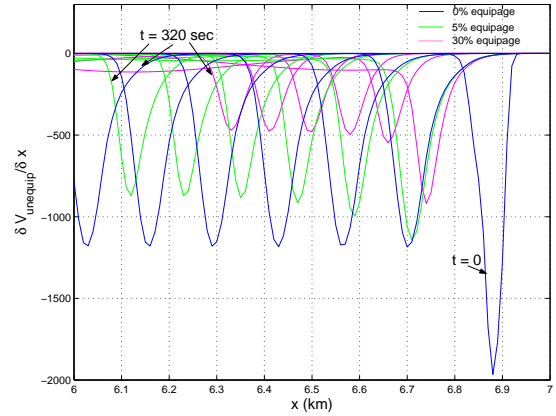


Fig. 14. $\frac{\partial V_u}{\partial x}$ for varying equipages for the Riemann Problem

$t = 0$ in the second. The reason that this case is interesting is because it enables us to see if and how varying equipage can arrest the formation of the discontinuity, before it has developed.

Figure 17 shows the average velocity profiles of the equipped and unequipped vehicles for the first scenario (assuming a 30% equipage). It is seen that the top portion of the average velocity (which had positive wave velocity when all vehicles were unequipped, i.e. it was moving forward relative to the highway), now immediately begins to move backwards as the communication wave passes through the equipped vehicles. This arrests the wave steepening effect that was present in the case of no equipage; and consequently the equipped vehicles do not experience any abrupt velocity gradient, while the unequipped vehicles experience a significantly reduced magnitude of negative velocity gradient, than they otherwise would have.

Figure 18 shows the time history of the magnitude of ΔV for the unequipped vehicles (for varying equipages), with ΔV representing the average velocity change of the unequipped vehicles over the region where $\frac{\partial V_{unequip}}{\partial x}$ is smaller than -100 kmph/km. It is seen that again a 5% equipage causes greatest reduction in ΔV and that above an equipage of 15%, the benefit obtained per unit increase in percentage equipage, is not significantly greater. The same effect is manifested in Figure 19 that shows $\|\frac{\partial V_u}{\partial x}\|_{\infty}$.

Figure 20 then shows the average velocity profile for the

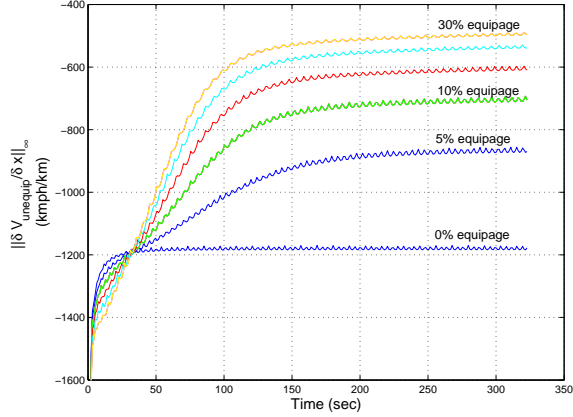


Fig. 15. $\|\frac{\partial V_u}{\partial x}\|_\infty$ for varying equipages for the Riemann Problem

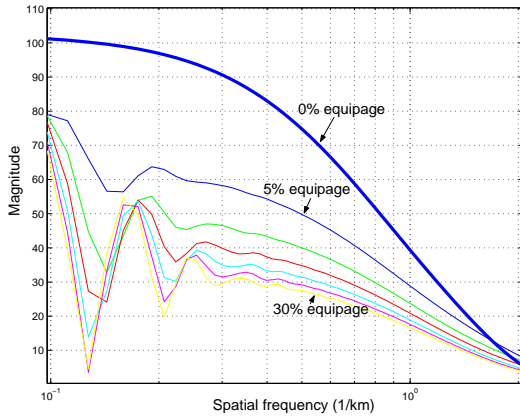


Fig. 16. Spatial frequency content of $\frac{\partial V_u}{\partial x}$ at $t = 320\text{sec}$ for different percentages of equipage for the Riemann Problem

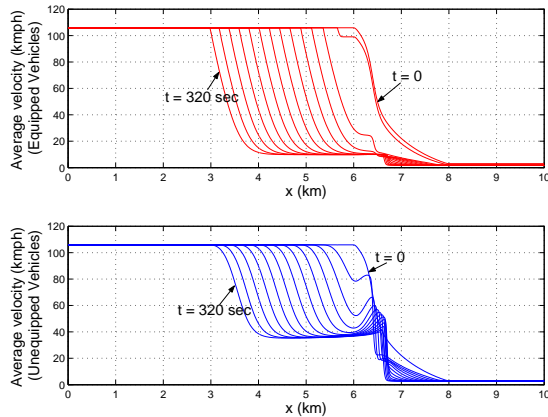


Fig. 17. Average velocity profiles of equipped and unequipped Vehicles (30% equipage) for the continuous initial condition (first information propagation scenario)

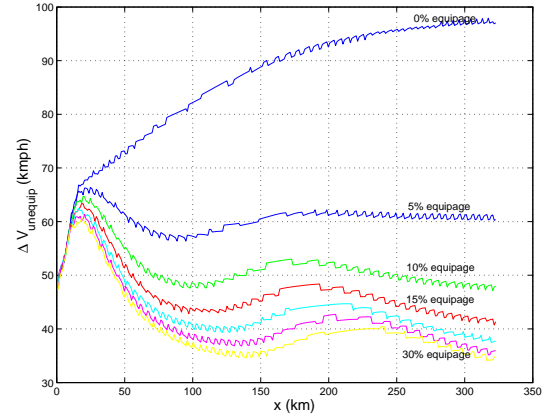


Fig. 18. Magnitude of ΔV_u for varying equipages for the continuous initial condition (first information propagation scenario)

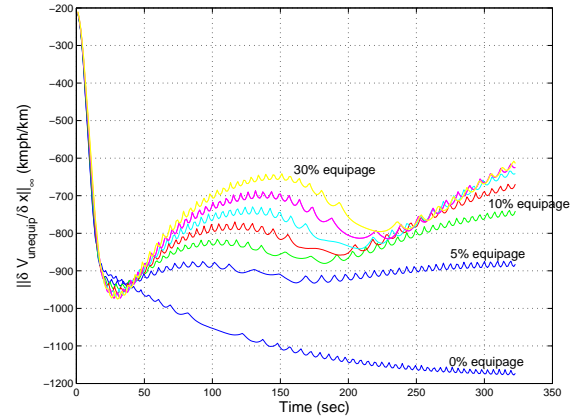


Fig. 19. $\|\frac{\partial V_u}{\partial x}\|_\infty$ for varying equipages for the continuous initial condition (first information propagation scenario)

same initial condition, but for the second scenario, i.e. we now assume that information of the low velocity originates from $x = 8\text{km}$, and this travels backwards at the communication speed of 25kmph . In this case, it is seen that the wave does steepen for a while - both the equipped and unequipped vehicles experience increasingly sharper negative velocity gradients for close to 3 minutes, before the smoothing effect of the slowdown warning system sets in. The reason that they experience the wave steepening for a while can be attributed to the fact that the top (high velocity) portion of the velocity wave continues to move forward for a while, before the communication wave comes upon it. This effect is also seen in Figure 21. This thus demonstrates that for this initial condition, a communication speed of 25 kmph is adequate if it originates from the left end of the velocity gradient (as in the first scenario), but it is inadequate if it originates from the right end of the velocity gradient (as in the second scenario).

IV. CONCLUSIONS

In this paper, the effect of a slowdown warning system on a macroscopic traffic model is analyzed. A slowdown warning system warns vehicles of the existence of large

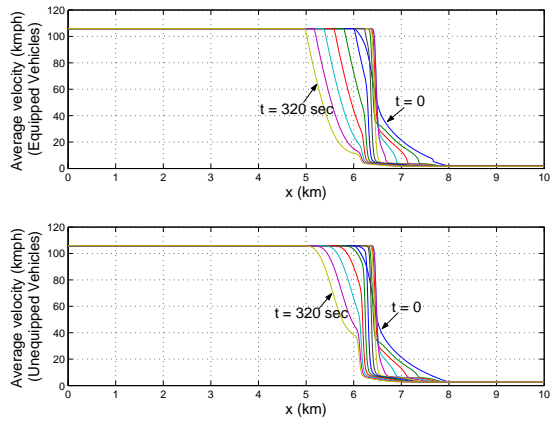


Fig. 20. Average velocity profiles of equipped and unequipped Vehicles (30% equipage) for the continuous initial condition(second information propagation scenario)

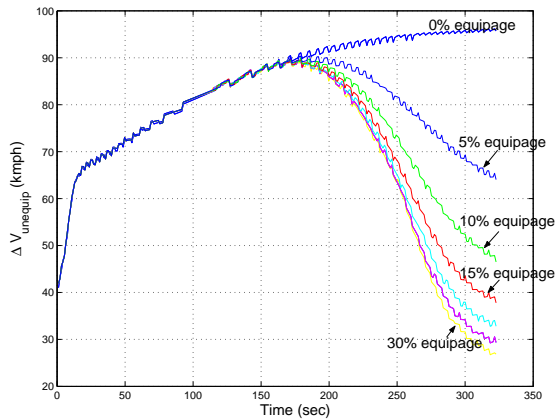


Fig. 21. Magnitude of ΔV_u for varying equipages for the continuous initial condition(second information propagation scenario)

negative velocity gradients/low velocities on the highway ahead, so the drivers can take anticipative action accordingly. Different types of initial conditions - those with initial large negative velocity gradients at the very outset, and those with initially mild velocity gradients that then propagate with time to become sharper and sharper, are examined. The effect of partial equipage of the slowdown warning system in these scenarios is studied, and the effect of varying equipage on the subsequent velocity gradients is analyzed.

V. ACKNOWLEDGMENTS

This work is supported by the National Science Foundation Award CCR-0208831, the Deshpande Center for Technological Innovation Award 009216-015 and the Ford-MIT Alliance Program.

REFERENCES

[1] CNN News, "Five seriously hurt in 194-vehicle California pileup," Nov. 3, 2002.
 [2] CNN News, "Massive pile-up near Ga.-Tenn. line kills 4," March 14, 2002.
 [3] Boston Globe News, "Sixty six vehicle California Pileup," April 2, 2004.

[4] Boston Globe News, "Rains trigger 30 car pileup on I-93," August 4, 2003.
 [5] P. I. Richards, "Shock Waves on the Highway," *Operations Research*, Vol. 4, No. 42, 1956, pp. 209-229.
 [6] M. H. Lighthill, G. B. Whitham, "On kinematic waves II : A theory of traffic flow on long, crowded roads," *Proc. Of the Royal Society of London Ser. A* 229, pp. 317-345, 1945.
 [7] H. J. Payne, "Models of Freeway Traffic and Control," *Simulation Council*, 1971.
 [8] G. B. Whitham, "Linear and Nonlinear Waves," *Wiley*, 1974.
 [9] J. K. Hedrick, R. Sengupta, Q. Xu, Y. Kang, C. Lee, "Enhanced AHS Safety Through the Integration of Vehicle Control and Communication," *California PATH Research Report UCB-ITS-PRR-2003-27*, September 2003.
 [10] A. R. Girard, J. B. de Sousa, J. K. Hedrick, "An Overview of Emerging Results in Networked Multi-Vehicle Systems," *Proc. of the 40th IEEE Conference on Decision and Control*, December 2001, pp. 1485-1490.
 [11] Q. Xu, K. Hedrick, R. Sengupta, J. VanderWerf, "Effects of Vehicle-vehicle/roadside-vehicle Communication on Adaptive Cruise Controlled Highway Systems," *Proc. of the 56th IEEE Vehicular Technology Conference*, Vol. 2, September 2002, pp. 1249-1253.
 [12] S. Kato, S. Tsugawa, K. Tokuda, T. Matsui, H. Fujii, "Vehicle control algorithms for cooperative driving with automated vehicles and intervehicle communications," *IEEE Transactions on Intelligent Transportation Systems*, Vol. 3, No. 3, September 2002, pp. 155-161.
 [13] J. Carbaugh, D. Godbole, R. Sengupta, "Safety and capacity analysis of automated and manual highway systems," *Transportation Research C* (6), 1998, pp. 69-99.
 [14] D. Helbing, A. Hennecke, V. Shvetsov and M. Treiber, "Micro- and Macro-Simulation of Freeway Traffic," *Mathematical and Computer Modelling* 35, 2002, pp. 517-547.
 [15] D. Helbing, "Gas-kinetic derivation of Navier-Stokes-like traffic equations," *Physical Review E* 53, March 1996, pp. 2366-2381.
 [16] M. Treiber, A. Hennecke and D. Helbing, "Derivation, properties and simulation of a gas-kinetic-based, nonlocal traffic model," *Physical Review E* 59, January 1999, pp. 239-253.
 [17] S. P. Hoogendoorn and P. H. L. Bovy, "Continuum modeling of multiclass traffic flow," *Transportation Research, Part B* 34, 2000, pp. 123-146.
 [18] I. Prigogine and R. Herman, "Kinetic theory of vehicular traffic," *Elsevier*, 1971.
 [19] S. L. Paveri-Fontana, "On Boltzmann like treatments for traffic flow," *Transportation Research Part B*, Vol. 9, pp. 225-235, 1975.
 [20] J. Yi, H. Lin, L. Alvarez and R. Horowitz, "Stability of Macroscopic Traffic Flow Modeling through Wavefront Expansion," *Transportation Research Part B*, 2003.
 [21] A. Bose, P. A. Ioannou, "Analysis of Traffic Flow with Mixed Manual and Semiautomated Vehicles," *IEEE Transactions on Intelligent Transportation Systems*, Vol. 4, No. 4, December 2003, pp. 173-188.
 [22] A. Bose, P. A. Ioannou, "Mixed manual/semi-automated traffic: a macroscopic analysis," *Transportation Research Part C* 11 (2003), pp. 439-462.
 [23] A. Chakravarthy, K.Y. Song, and E. Feron, "A GPS-based slowdown warning system for automotive safety," *Proc. of IEEE Intelligent Vehicles Symposium*, June 14-17, 2004, Parma, Italy, pp. 489-494.
 [24] A. Chakravarthy, K.Y. Song, and E. Feron, "A slowdown warning system for automobiles," *Proc. of IEEE SMC*, October 10-13, 2004, The Hague, Netherlands.
 [25] A. Chakravarthy, K.Y. Song, E. Feron, "Influence of a slowdown warning system on a multi-vehicle stream," *Proc. of American Control Conference*, June 8-10, 2005, Portland.